Electrochemical chloride extraction to repair combined carbonated and chloride contaminated reinforced concrete

Yolaine Tissier, Véronique Bouteiller, Elisabeth Marie-Victoire, Suzanne Joiret, Thierry Chaussadent, Yunyun Tong

Electrochemical chloride extraction to repair combined carbonated and chloride contaminated reinforced concrete

Yolaine Tissier [1-4], Véronique Bouteiller [1,*], Elisabeth Marie Victoire [2,3], Suzanne Joiret [4], Thierry Chaussadent [5] and YunYun Tong [1-4, +]

[1] Université Paris-Est, MAST, EMGCU, IFSTTAR, F-77447 Marne-la-Vallée, France

[2] Laboratoire de recherche des monuments historiques, Ministère de la Culture, 29 rue de Paris, 77420 Champs-sur-Marne, France

[3] Centre de recherche sur la conservation (CRC), Muséum national d'histoire naturelle, CNRS, ministère de la Culture, 36 rue Geoffroy St Hilaire, 75005 Paris, France

[4] UPMC Université Paris 06, Sorbonne Université, UMR 8235, Laboratoire Interfaces & Systèmes Electrochimiques, F-75005 Paris, France.

[5] Université Paris-Est, MAST, CPDM, IFSTTAR, F-77447 Marne-la-Vallée, France

+ Present address: Zhejiang University of Science & Technology, School of Civil Engineering & Architecture, No.318# LiuHe Road, Hangzhou, China

Abstract

The increasing international interest in contemporary architecture has drawn attention to the numerous listed buildings made of reinforced concrete in Europe, and especially in France. The main source of deterioration of this cultural heritage is the corrosion of rebars through carbonation or chloride contamination, but also often by a combination of both. The present study explored this combined corrosion mechanism in reinforced concretes, and investigated Electrochemical Chloride Extraction (ECE) as a technique to stop or decrease corrosion. The analytical approach was based on physico-chemistry, electrochemical measurements, Raman spectroscopy and SEM examinations. The results evidenced the aggressiveness of the combined carbonation and chloride-induced corrosion, and demonstrated the efficiency of the ECE treatment in terms of chloride extraction and reduction of corrosion rate. It appears that ECE treatment only reduces corrosion activity by increasing pH to a value of 10. Nevertheless, the long term durability of the treatment is questionable as the return to a sound concrete passivity is not obtained.

Keywords

Electrochemical chloride extraction; reinforced concrete; carbonation; Raman micro-spectroscopy

1 Introduction

Concrete is now part of the world cultural heritage landscape, as evidenced by the recent Unesco listing of the famous German Bauhaus architecture, the Polish Centennial Hall in Warsaw and the center of the French city Le Havre (rebuilt by Auguste Perret) for their outstanding universal value [1].

The Redmonest European Project revealed that at least 1500 buildings made of concrete are now registered in Belgium, France, and Spain. The survey performed within the project shows that the protection of this contemporary heritage is exponential in France, where the number of listed concrete monuments increased from 200 in the 1990's to more than 800 in the 2010's [2, 3].

This architectural heritage is unfortunately affected by several types of deterioration, the most deleterious of which is certainly rebars corrosion. Several phenomena are involved in this process. The oldest of these historic concretes were cast at a time when mix design or casting were still a new and developing technology, meaning that poor initial concrete quality or insufficient concrete covers can sometimes be encountered. It is usual to measure carbonation depth of several centimeters in concrete made in the 1920s or 1940s, with open porosity of up to 20% [4, 5]. When those carbonated concretes are subjected to marine chlorides or to de-icing salts, the double contamination can contribute to severe corrosion. In historic concrete, this leads to a massive and unacceptable loss of original materials.

The standard technique to cure this deterioration is patch repair. However, the 2007 CONREPNET European project showed that patches for repairing reinforced concrete corrosion were not efficient over time [6]. Among the reasons for this lack of durability, the compatibility of the patch materials with the parent historic concrete

was the main reason for early failure (within 2 years). The authors suggest that longer term failure could be attributed to the location of the repair patch, which only concerns the spall area and not the surrounding concrete, which is still carbonated or chloride polluted. There was therefore a need for additional treatments to address degradations induced by corrosion. Electrochemical realkalization and chloride extraction were studied for this purpose [7-11].

Corrosion has been extensively studied in chloride-polluted concrete [12-22] or in carbonated reinforced concrete [23, 24], but the combined effect of the two contaminants has rarely been investigated.

The primary aim of the present study was to investigate the corrosion mechanism resulting from combined carbonation and chloride contaminations. This issue was explored using artificially carbonated concrete with either endogenous (chloride added to the mix) or exogenous (wet and dry cycles) chlorides.

In a second step, an electrochemical chloride extraction was studied. Chloride content, pH evolution, and corrosion rates were characterized. Special attention was paid to the evolution of corrosion products during treatment using an analytical approach that combined Raman micro-spectroscopy and SEM observations.

2 Materials and methods

2.1 Samples and ageing procedures

The reinforced micro-concrete samples were cylinders (10 cm high and 4 cm diameter) with a central rebar. Two cements were studied, namely an ordinary Portland cement (CEM I) and a blast furnace slag cement (CEM III/A). These two cements are of interest: the former was widely used for many years, and the latter was extensively used between the two world wars and its use is currently increasing.

Rebar was composed of smooth carbon steel with a diameter of 5 mm and an active surface of 10cm² delimited with cataphoretic paint (Fig. SI1-1). A rather high water/cement ratio (0.65) was used for concrete formulation to obtain high porosity and thus accelerate the ingress of contaminants (carbonation and chloride ions). This high water/cement ratio is representative of the ratio used in historic concretes.

Four sample series were prepared based on two criteria, namely:

- Contamination content, i.e. either chlorides added to the mix and followed by carbonation (referenced G), or carbonation followed by wetting/drying cycles in a salted solution (referenced I), and
- Cement type (CEM I or CEM III/A, respectively referenced 1 and 3).

Therefore, four series named G1, G3, I1, and I3 were studied

A precise description of the sample production and contamination can be found in Supplementary Information 1.

2.2 Electrochemical chloride extraction

The electrochemical chloride extraction (ECE) treatment is illustrated in Figure 1. ECE was conducted on 37 specimens of each sample series. A cathodic current density of -100 µA/cm² of steel was applied with a power supply between the rebar and a titanium/platinum grid (counter-electrode) for 8 weeks, corresponding to a total charge of 1344 A.h/m². These current density and duration conditions are in accordance with those reported in the technical specification or standards for chloride extraction [25] and realkalization [26]. A disodium tetraborate solution (25g/L of $Na_2B_4O_7$ $10H_2O$) electrolyte was used as a 9 pH buffer corresponding to a carbonated concrete. Moreover, some samples were immersed in the electrolyte then

studied to evaluate the lixiviation of chloride ions without current (no polarization). Three samples from each series were analyzed after 3, 7, 14, 28, and 56 days of treatment: two were dedicated to destructive analysis and the third was used for non-destructive electrochemical characterizations.

2.3 Analytical techniques

2.3.1 Phenolphthalein test

Phenolphthalein (0.5 % in ethanol) was used to determine realkalization progress during the treatment. A pink color is obtained for a pH of 9 or more, whereas the concrete remains colorless for lower pH values.

2.3.2 Chloride titration

Regarding the chloride extraction evolution, the free and total chloride contents of concrete were measured by $AgNO_3$ potentiometric titration [27-28] on the first centimeter around the rebar on two of the three samples. The free and total chloride contents of concrete were simultaneously determined on the non-polarized samples after 14, 28 and 56 days.

2.3.3 Electrochemical characterizations

Electrochemical characterizations were conducted at each step of the set-up: after curing, after ageing (chloride or carbonation or reverse) and during ECE treatment (depending on the treatment duration). Linear polarization resistance (LPR) and electrical concrete resistance Re were measured using a 5-channel Bio-Logic VMP2Z potentiostat (details in SI2). Corrosion rate i_{corr} (µA/cm² of steel) was calculated according to the Stern-Geary equation (Eq.1)

$$i_{corr} = B/(Rp.S) \qquad \text{(Eq. 1)}$$

Where [29]: B = 26 mV, Rp (ohm) is obtained from the linear polarization resistance and the electrical concrete resistance (Re), and S is the active steel surface (10 cm² in this study).

2.3.4 Raman micro-spectroscopy

The Raman spectrometer equipment was a HORIBA Jobin Yvon LABRAM consisting of an Olympus BX40 microscope confocally coupled to a 300 mm focal length spectrograph. The latter was equipped with a holographic grating (1800 grooves/mm) and a Peltier-cooled CCD detector (1024 × 256 pixels). The spectra were obtained with 632.817nm radiation from an internal 10mW HeNe laser with neutral density filters and 0.7mW attaining the surface of the sample to avoid any thermal effect. For *in situ* studies, a 50× ULWD (Ultra-Long Working Distance) allows the recording of Raman spectra with a working distance of 8 mm.

Electrodes for *in situ* Raman spectroscopy were specially designed for this study. As shown in Figures SI1-2, Raman spectroscopy samples were cut from double-contaminated concrete samples. A glass window was glued on top of the freshly polished sample shortly before the experiment, as represented in Figure 2. The electrode was immersed window-up in disodium tetraborate solution with 5mm left outside the electrolyte to ensure that the steel was polarized in a pore solution that had to cross 17.5 mm of concrete and had no direct contact with the atmosphere. Spectra were recorded solely at the rebar concrete interface. Spectra during corrosion initiation were obtained at open circuit potential. Treatment was then applied with an Autolab galvanostat using the same current density (-100 µA/cm^2) as previously described. Spectra were then recorded for each sample subjected to cathodic polarization.

3 Results and discussion

3.1 Initial characterizations

Table 1 shows the characterizations of chloride content, pH, and corrosion rate before treatment.

Levels of chloride content in the samples were sufficiently high compared to critical content to induce corrosion [30] and was found to be within the range of chloride threshold provided in states of the art [12, 13].

The pH value of the 17.5 mm concrete cover was close to 9 (phenolphthalein was colorless) demonstrating the complete carbonation of the concrete samples [31-33].

Corrosion rates indicated a passive state for sound concrete. However, corrosion current in the carbonated and chloride-contaminated samples was close to 10 µA/cm² for all four series, and corresponded to a high level of corrosion in reinforced concrete [29]. This value was higher than those observed in samples with a single contaminant, and highlighted the aggressiveness of the combined contamination (Table 1).

3.2 Chloride extraction

During the ECE treatment, the negatively charged chloride ions migrated from the rebar to the electrolyte. The efficiency of the electrochemical chloride extraction treatment was considered to be the ratio of the initial chloride content minus the remaining chloride content (after each duration time) divided by the initial chloride content. Figure 3 presents the results of the chloride extraction efficiency versus treatment duration for the I1 series and for the corresponding non-polarized samples. Chloride ions were in a free form because carbonation induced a release of bonded chlorides (as evidenced by the free and total chlorides content values, which are

similar in Figure 3). As the four series all showed the same behavior, the results of the three other series can be found in Figure SI3.

For the treated samples, an increase of extracted chloride content with increased treatment duration was observed for the four series. Moreover, the extraction was found to be more efficient during the initial stage of the treatment, as previously described by different authors [34-36]. After 28 days, the efficiency of the extraction was close to 90% for G1, G3 and I1 and was close to 75% for I3 samples (Figure 3 and Figure SI3-1). These high extraction efficiencies can be explained by a porous and thin concrete cover, and by chloride ions that are likely in the free form. The extraction of chloride ions was also observed for the non-polarized samples, but was attributed to a lixiviation phenomenon.

Chloride extraction resulting from the electrochemical treatment was faster than the lixiviation phenomenon (similar values were obtained only after 56 days).

In an *in situ* situation involving better quality concrete with better quality (thicker and/or less porous), ECE treatment would require a longer duration. In this case, the end of the treatment correspond to the attaining of a chloride content target, for example.

3.3 pH evolution

During treatment, water hydrolysis leads to hydroxyl ion formation. An increase of concrete pH around the rebar is therefore expected. Figure 4a presents the results of the pH evolution (pink ring thickness) versus treatment duration for the four series. Figures 4b and 4c show pictures of the phenolphthalein color after 28 and 56 days for I1 series. The thickness of the realkalized concrete around the rebar increased with time. According to [26], the treatment is efficient if the realkalized concrete around the

rebar is equal to the diameter of the rebar if the latter measures less than one centimeter in diameter, or 1 cm for larger rebar diameters. The results shown in Figure 4a demonstrate that the realkalization was efficient after 14 days for all four series: the ring thickness was larger than the 5 mm rebar diameter. After 56 days of treatment, it was equal to 9, 10, 12 and 14 mm respectively for G3, G1, I1, and I3 series., As expected, no realkalized ring was observed for the non-polarized samples.

3.4 *In situ* Raman micro spectroscopy

Before treatment, an induction time of 12 hours to 5 days was compulsory to obtain active corrosion around the rebar after immersion in tetraborate solution. Control of the corrosion current gave the same order of magnitude (10 to 50 µA/cm^2) as those observed in previously described samples. The higher values were attributed to the rebar cross section that was also exposed to the pore solution.

Raman spectra obtained at this stage are reported on Figure 5a and 5c with reference Raman spectra of Green Rust (GR) grown respectively in chloride (Figure 5b) or carbonate (Figure 5d) solution according to the protocols described in SI1-2. The four series tested mainly showed spectrum 5a, while some spots on G1 samples indicated spectrum 5c.

The main differences between the two types of Green Rust spectra are the gap and the position between the two main bands, which are respectively 70 cm^{-1} [500-430] for GR(Cl^-) and 75 cm^{-1} [510-435] for GR(HCO_3^-), and the presence of two smaller bands at 320 and 360 cm^{-1} for GR(Cl^-). Clearly spectrum a) is linked to GR(Cl^-) ; while spectrum 5c is attributed to GR(CO_3^{2-}).

The presence of these compounds attests a fast corrosion process in which chloride is incorporated within corrosion products as the anions in Green Rust structure to counterbalance the presence of iron III. GR(Cl^-) are known to be thermodynamically unfavored compared to carbonate (or sulphate)-based GRs [37]. The localized observation of GR(CO_3^{2-}) on G samples shows inhomogeneous distribution of chloride ion concentration in pore solution.

The stability of GR spectra over several days also shows that our setup efficiently protects the concrete rebar interface from atmospheric oxidation. This reflects the situation in real concrete, where oxygen penetration is a slow process [38].

During treatment, once corrosion was proved to occur by the formation of spots of Green Rust, a cathodic current of -100 µA/cm^2 was added to the system. Raman spectra were periodically recorded during this treatment. The spectra observed during the reduction process are depicted in Figure 6 for I1 sample.

After polarization is turned on, the characteristic band of magnetite Fe_3O_4 appears at 670 cm^{-1}. With time, a progressive increase is observed in magnetite bands, causing a decrease in Green Rust bands until they almost completely disappear. All the studied series behaved in the same manner, the only differences being the induction time and the growing rate of magnetite, which both varied from one sample to the other (SI 4). However, magnetite was the predominant band for all samples after 24 hours of polarization.

After longer polarization time (more than one day), new Raman spectra were recorded for a few spots around the rebar. They are depicted in Figure 7a for I1 sample and in Figure 7b for G3 sample. Similar behavior was also recorded for I3 sample (not shown). No information was obtained for G1 sample after 24 hours due

to a high interface fluorescence. Figure 7a presents the evolution of the Green Rust bands, with a rapid decrease in the intensity of the 500 cm^{-1} band compared that of the 430 cm^{-1} band. A shift of the 430 cm^{-1} band towards a lower wavenumber (410 cm^{-1}) is also observed. Moreover, after 2 days a new band appears in the 3600 cm^{-1} range (see insert in Figure 7a) corresponding to O-H stretching vibration at 3575 cm^{-1}. These values were in accordance with reference [39] and indicated the formation of $Fe(OH)_2$ in I1 series. In Figure 7b, after 3 days of treatment, two new bands appeared in the Raman spectrum: 205 cm^{-1} and 280 cm^{-1}. They correspond to mackinawite $Fe_{1-x}S$ [40] in G3 series (also observed for I3 series, not shown). The presence of sulfide is due to the blast furnace material contained in cement 3 (CEM III/A) [22].

In situ Raman spectroscopy analysis of the chloride extraction treatment made it possible to collect information on corrosion mechanisms. First, as expected in a medium pH range containing anions such as chloride, carbonate, or sulfate, rebar corrosion takes place through the formation of Green Rust [41]. This iron II hydroxide-based compound contains some iron III ions, and the balanced charge is compensated with anions originating from the solution, mainly chlorides in this case.

A progressive transformation of Green Rust into magnetite was evidenced during cathodic polarization, as pH in the pore solution near the rebar increases due to the reduction process. The literature indicates that a pH of around 10-11 is necessary for this transformation to take place [42]. Raman spectroscopy showed this process to be relatively fast compared to the treatment duration, and also evidenced the rapid release of chloride anions inserted in corrosion products.

However, the local formation of iron II compounds that can be easily oxidized [39-40, 43], (hydroxide in CEM I and sulfide in CEM III/A) during long polarization durations, while GR and magnetite are hardly visible in the Raman spectra, is a clear indication of corrosion that is still active in some spots around the rebar.

3.5 Corrosion rate

ECE treatment aims to decrease or even stop reinforcement corrosion. Figure 8 presents the results of corrosion rates versus treatment duration. These measurements were performed 3 months after the end of the treatment period in order to allow the system to recover a stable state (with the exception of time 0). For the four series, the ECE treatment leads to a decrease of the corrosion rates over time, with two or three orders of magnitude (log scale). From days 14 to 56 of treatment (corresponding to durations after which free chloride content was below 0.4%), corrosion rates decreased to values below 0.1 µA/cm².

Corrosion rates remained in the range 1 to 10 µA/cm² in the non-polarized samples, where chloride ions had been removed by lixiviation but were still carbonated.

These results show that chloride extraction and pH increase are both needed to slow down the corrosion of the reinforcement and that realkalization is mandatory.

Raman spectroscopy shows that the chloride ions that are bonded to the corrosion products were released at the beginning of the cathodic treatment and were therefore completely extracted. On the lixiviated samples, the chlorides that were bonded to the corrosion products remained at the rebar/concrete interface. They can be released by the oxidation of GR into iron III oxyhydroxides, and can thus cause further corrosion.

Nevertheless, corrosion rates for after treatment remained one order of magnitude higher than for the sound concrete for all contaminated samples. The passive state of the rebar in the sound concrete was not therefore recovered in the samples. This was confirmed by the presence of iron II revealed by Raman spectroscopy, indicating that corrosion was still active on some spots.

3.6 Durability

In a previous study dealing with an impressed current realkalization treatment applied to carbonated reinforced concrete, the pH increased from 9 to 10-11 after treatment (quantitative pH determination from powders in solution), inducing a decrease in the corrosion rates [44, 45]. Although the pH remained constant with time, corrosion rates gradually increased again, and finally reached the corrosion rate values observed for untreated carbonated reinforced concrete 30 months after the end of treatment. This behavior was explained by the fact that the increase in pH was not sufficient, as the sound pH concrete value of 13 was not recovered [45]. Identical cement (CEM I) and mortar composition and similar experimental conditions were used in this previous study and in the present study. Based on this, the hypothesis of similar behavior can be assumed. Moreover, Tlili et al. [46] observed a limit for the pH increase in carbonated solution due to a buffer effect. Figure 9 presents SEM observations of realkalized samples thirty months and five years after treatment. They exhibit a doubling of the corrosion layer thickness (15 to 30 µm) over time (30 to 60 months), evidencing a reactivation of corrosion.

Therefore, although the electrochemical treatment applied to reinforced concrete with a double contamination seems to be efficient in extracting chlorides and reducing reinforcement corrosion, the long-term efficiency with regard to pH evolution needs to be examined in greater detail.

4 Conclusions

This study considers rebar corrosion in combined carbonated and chloride contaminated concrete. The aggressiveness of the combined contaminants compared to that of a single one (carbonation or chloride ions) was highlighted by corrosion rate results and the detection of chlorides in Green Rust by *in situ* Raman spectroscopy.

Whatever the cement type and the contamination mode, the efficiency of electrochemical chloride extraction treatment was demonstrated by 90% chloride extraction and a decrease of the corrosion rate by three orders of magnitude. An increase of pH up to a value of 10 was also observed. The same amount of chlorides was extracted in ECE-treated samples and non-polarized lixiviated samples, but the corrosion rate retained its initial value in the latter. This shows that a pH increase is mandatory to reduce corrosion. At a microscale, this can be related to the transformation of Green Rust into magnetite, as observed by Raman spectroscopy during the treatment. This pH-driven modification released chloride anions that were bonded to the corrosion products.

However, the long-term durability of the treatment is uncertain. Corrosion rate decrease and pH increase did not reach the respective sound concrete values. The presence of iron II compounds casts doubt on the passivity of the rebar.

This primary aim of this study was to find a restoration solution for historic concretes affected by both carbonation and chloride contamination than can also be used for civil engineering structures. In the latter case, permanent Impressed Current Cathodic Protection (ICCP) can be easily implemented to stabilize the corrosion

decrease. The invasiveness and the irreversibility of the ICCP treatment are a challenge in the preservation of historic concretes.

Acknowledgements

Funding for this work was provided by the French Ministries of Culture, Environment, Research and Education.

References

[1] Site web [https://whc.unesco.org/fr/list/1181]

[2] E. Marie-Victoire, M. Bouichou, T. Congar, R. Blanchard, Concrete cultural heritage in France: inventory and state of conservation, 4th international conference on concrete Repair, Rehabilitation and Retrofitting (ICCRRR-4), Concrete repair, rehabilitation and retrofitting IV, Leipzig, Germany, (2015) 343-350.

[3] E. Marie-Victoire, M. Bouichou, H. Jourdan, Water-repellents as alternative carbonation-induced corrosion treatments for reinforced concrete cultural heritage 14th international conference on durability of buildings materials and components (DBMC), Ghent, Belgium, (2017) 399.

[4] M. Hergenroeder, R. Rackwitz, Investigations on the statistics of carbonation depths in concrete, 2nd International RILEM/CEB symposium on quality control of concrete structures, Ghent, Belgium, (1991) 42-47.

[5] E. Marie-Victoire, E. Cailleux, A. Texier, Carbonation and historical buildings made of concrete, NUCPERF 2006: Corrosion and long term performance of

concrete in NPP and waste facilities, Journal de physique IV, Cadarache, France, (2006) 305-318.

[6] G.P. Tilly, J. Jacobs, CONREPNET - Concrete repairs - Performance in service and current practice, IHS BRE Press, United Kingdom, (2007).

[7] D. Pocock, Chloride extraction and realkalization - six years on, Corrosion and protection of reinforced concrete, Dubai, (1994).

[8] D. Pocock, Chloride extraction and realkalization - six years on, Construction Repair, Concrete Repairs, 9 (1995) 42-47.

[9] L. Bertolini, M. Carsana, E. Redaelli, Conservation of historical reinforced concrete structures damaged by carbonation induced corrosion by means of electrochemical realkalization, Journal of Cultural Heritage, 9 (2008) 376-385.

[10] J. Mietz, Electrochemical realkalization for rehabilitation of reinforced concrete structures, Materials and Corrosion, 46 (1995) 527-533.

[11] J. Mietz, Electrochemical rehabilitation methods for reinforced concrete structures – a state of the art report. EFC N°24, I OM Communications Ltd, London, 1998.

[12] U. Angst, B. Elsener, C.K. Larsen, Ø. Vennesland, Critical chloride content in reinforced concrete - A review, Cement and Concrete Research, 39 (2009) 1122-1138.

[13] C. Alonso, C. Andrade, M. Castellote, P. Castro, Chloride threshold values to depassivate reinforcing bars embedded in a standardized OPC mortar, Cement and Concrete Research, 30 (2000) 1047-1055.

[14] O. Poupard, A. Aït-Mokhtar, P. Dumargue, Corrosion by chlorides in reinforced concrete: Determination of chloride concentration threshold by impedance spectroscopy, Cement and Concrete Research, 34 (2004) 991-1000.

[15] R.E. Melchers, I.A. Chaves, A comparative study of chlorides and longer-term reinforcement corrosion, Materials and Corrosion, 68 (2017) 613-621.

[16] V. Bouteiller, E. Marie-Victoire, C. Cremona, Mathematical relation of steel thickness loss with time related to reinforced concrete contaminated by chlorides, Construction and Building Materials, 124 (2016) 764-775.

[17] C. Arya, Y. Xu, Effect of cement type on chloride binding and corrosion of steel in concrete, Cement and Concrete Research, 25 (1995) 893-902.

[18] G.K. Glass, N.R. Buenfeld, The influence of chloride binding on the chloride induced corrosion risk in reinforced concrete, Corrosion Science, 42 (2000) 329-344.

[19] K.Y. Ann, H.-W. Song, Chloride threshold level for corrosion of steel in concrete, Corrosion Science, 49 (2007) 4113-4133.

[20] U. Angst, B. Elsener, C.K. Larsen, Ø. Vennesland, Chloride induced reinforcement corrosion: Rate limiting step of early pitting corrosion, Electrochimica Acta, 56 (2011) 5877-5889.

[21] B. Pradhan, B. Bhattacharjee, Rebar corrosion in chloride environment, Construction and Building Materials, 25 (2011) 2565-2575.

[22] V. Bouteiller, C. Cremona, V. Baroghel-Bouny, A. Maloula, Corrosion initiation of reinforced concretes based on Portland or GGBS cements: Chloride contents and electrochemical characterizations versus time, Cement and Concrete Research, 42 (2012) 1456-1467.

[23] M. Stefanoni, U. Angst, B. Elsener, Corrosion rate of carbon steel in carbonated concrete – A critical review, Cement and Concrete Research, 103 (2018) 35-48.

[24] G.K. Glass, C.L. Page, N.R. Short, Factors affecting the corrosion rate of steel in carbonated mortars, Corrosion Science, 32 (1991) 1283-1294.

[25] CEN/TS 14038-2:2011, Electrochemical re-alkalization and chloride extraction treatments for rein-forced, Concrete Part 2: Chloride extraction

[26] NF EN 14038-1:2016, Electrochemical realkalization and chloride extraction treatments for reinforced concrete - Part 1: Realkalization

[27] M. Castellote, C. Andrade, RILEM TC 178-TMC : Testing and modelling chloride penetration in concrete - Round robin test on chloride analysis in concrete Part 1 : Analysis of total chloride content, Materials and Structures, 34 (2001) 532 (Procedure A533-C534*).

[28] M. Castellote, C. Andrade, RILEM TC 178-TMC : Testing and modelling chloride penetration in concrete - Round robin test on chloride analysis in concrete Part 2 : Analysis water soluble chloride content, Materials and Structures, 34 (2001) 589 (Procedure B581).

[29] C. Andrade, C. Alonso, RILEM TC 154-EMC:Electrochemical Techniques for Measuring Metallic Corrosion - Recommendations - Test methods for on-site corrosion rate measurement of steel reinforcement in concrete by means of the polarization resistance method, Materials and Structures, 37 (2004) 623-643.

[30] AFNOR, NF EN 206-1 / P18-325-1. Béton : spécification, performances, production et conformités, (2004).

[31] A. Bentur, S. Diamond, N.S. Berke, Steel corrosion in concrete - Fundamentals and civil engineering practice, E&FN SPON, London, United Kingdom, (1997).

[32] J.P. Broomfield, Corrosion of steel in concrete - Understanding, investigation and repair, E&FN SPN, London, (1997).

[33] L. Bertolini, B. Elsener, P. Pedeferri, R. Polder, Corrosion of steel in concrete: prevention, diagnosis, repair, Wiley Vch Verlagsgesellschaft Mbh, Weinheim, (2004).

[34] J.C. Orellan Herrera, G. Escadeillas, G. Arliguie, Electrochemical chloride extraction: Influence of C3A of the cement on treatment efficiency, Cement and Concrete Research, 36 (2006) 1939-1946.

[35] R.N. Swamy, S. McHugh, Effectiveness and structural implications of electrochemical chloride extraction from reinforced concrete beams, Cement and Concrete Composites, 28 (2006) 722-733.

[36] G. Fajardo, G. Escadeillas, G. Arliguie, Electrochemical chloride extraction (ECE) from steel-reinforced concrete specimens contaminated by "artificial" sea-water, Corrosion Science, 48 (2006) 110-125.

[37] M. Abdelmoula, P. Refait, S. H. Drissi, J. P. Mihe, and J.-M. R. Genin. Conversion electron Moessbauer spectroscopy and x-ray diffraction studies of the formation of carbonate-containing Green Rust one by corrosion of metallic iron in NaHCO3 and (NaHCO3 + NaCl) solutions. Corrosion Science 38, (1996) 623-633.

[38] N. Boucherit, A. Hugot-Le Goff, and S. Joiret. Raman studies of corrosion films grown on iron and iron-molybdenum (Fe-6Mo) in pitting conditions. Corrosion Science 32, (1991) 497-507.

[39] H. D. Lutz, H. Moeller, and M. Schmidt. Lattice vibration spectra. Part LXXXII. Brucite-type hydroxides M(OH)2 (M = Ca, Mn, Co, Fe, Cd) - IR and Raman spectra, neutron diffraction of Fe(OH)2. Journal of Molecular Structure 328, (1994) 121-132..

[40] J.A. Bourdoiseau, M. Jeannin, R. Sabot, C. Rémazeilles, and P. Refait, Characterisation of mackinawite by Raman spectroscopy: Effects of cristallisation, drying and oxidation. Corrosion Science 50 (2008) 3247-3255.

[41] P Refait, M Jeannin, R Sabot, H Antony, S Pineau, Corrosion and cathodic protection of carbon steel in the tidal zone: Products, mechanisms and kinetics Corrosion Science 90 (2015) 375-382

[42] A. Sumoondur, S. Shaw, I. Ahmed, and L. G. Benning. Green Rust as a precursor for magnetite: an *in situ* synchrotron based study. Mineralogical Magazine 72[1], (2008) 201-204.

[43] J.A. Bourdoiseau, M. Jeannin, C. Rémazeilles, R. Sabot and P. Refait, The transformation of mackinawite into greigite studied by Raman spectroscopy. Journal of Raman Spectroscopy, 42 (2010) 496-504.

[44] Y.Y. Tong, V. Bouteiller, E. Marie-Victoire, S. Joiret, Efficiency investigations of electrochemical realkalization treatment applied to carbonated reinforced concrete — Part 1: Sacrificial anode process, Cement and Concrete Research, 42 (2012) 84-94.

[45] M. Sahal, Y.Y. Tong, B. Sanz-Merino, V. Bouteiller, E. Marie-Victoire, S. Joiret, Durability of impressed current realkalization treatment applied on reinforced concrete slabs after 5 Years DBMC Porto, Portugal (2011) (https://www.irbnet.de/daten/iconda/CIB22511.pdf)

[46] M.M. Tlili, M. Benamor, C. Gabrielli, H. Perrot, B. Tribollet, Influence of the interfacial pH on electrochemical CaCO3 precipitation, Journal of the electrochemical society, 150 11 (2003) C765-C771

Figure captions

Figure 1: Electrochemical chloride extraction set-up.

Figure 2: Top view of the electrode with glass used for in situ Raman spectroscopy.

Figure 3: Free ■ and total ▲ fraction of extracted chlorides for the internal part during treatment and free □ and total △ fraction of extracted chlorides for the internal part of the non-polarized samples versus treatment duration for I1 series.

Figure 4: Diameter of realkalized concrete around the rebar versus treatment duration for ■ G1, □ I1, ● G3, ○ I3 series (a) and examples of phenolphtalein test for I1 samples ((b) 28 and (c) 56 days).

Figure 5: a), c) In situ Raman spectra of the metal concrete interface after immersion in tetraborate solution; b) reference Raman spectrum of GR(Cl^-) and d) reference Raman spectrum of GR(CO_3^{2-})

Figure 6: In situ Raman spectra evolution with polarization time , 600s exposure time, a spectrum every 13 minutes, spectra have been offset for sake of clarity. I1 series, tetraborate solution, cathodic current I=-100µA/cm^2

Figure 7: In situ Raman spectra evolution with long polarization time; spectra have been offset for sake of clarity, tetraborate solution, cathodic current I=-100µA/cm^2, a) I1 series inset: O-H stretching range and b) G3 series

Figure 8: Corrosion current for ●G1, ■G3, ▼ I1▲ I3 series polarized in tetraborate solution and ○G1, □G3, ▽I1 △I3 non polarized sample versus treatment duration.

Figure 9: Corrosion products layers after the realkalization treatment a) 30 months after (thickness = 15µm) and b) 60 months after (thickness = 30µm). R: rebar, C: concrete

Table 1: Characterizations before treatment: corrosion rate (µA/cm²), pH value and chloride content (% weight of cement) for the four series.

series	sound concrete	Cl^- contaminated	CO_2 contaminated	Cl^- +CO_2 contaminated		
	Icorr/ µA.cm^{-2} (standard deviation)				pH	Free chloride content (% weight of cement)
G1	0.00	0.02		10.99 (1.82)	9	1.4
I1	0.00		2.72	9.34 (3.27)	9	0.9
G3	0.01	0.06		7.82 (1.07)	9	2.1
I3	0.01		8.80	9.39 (4.87)	9	1.1

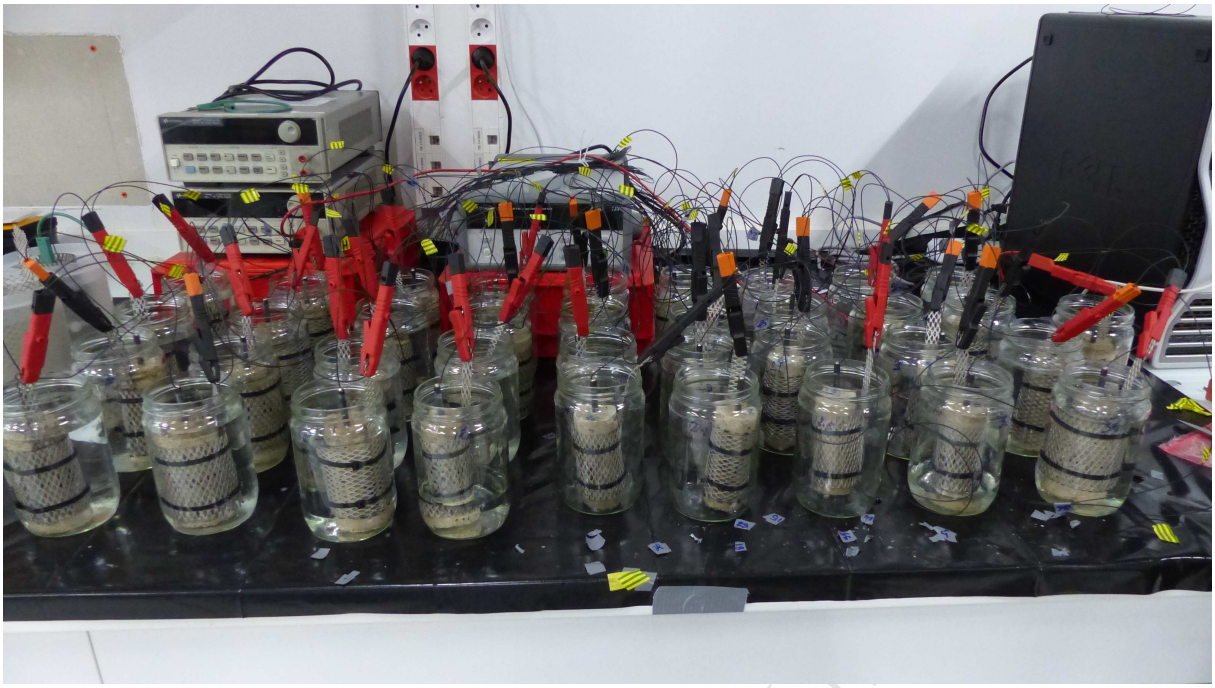

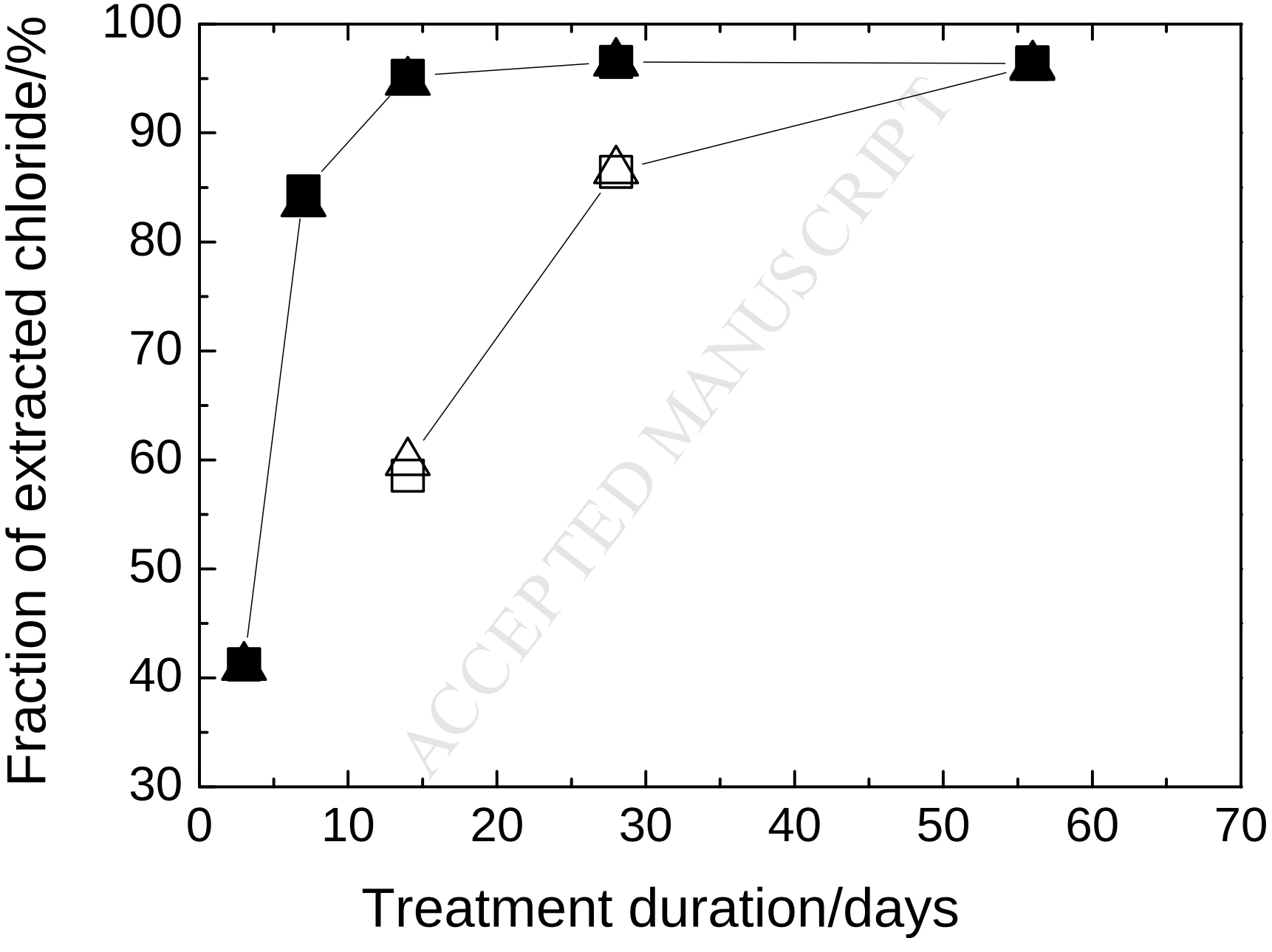

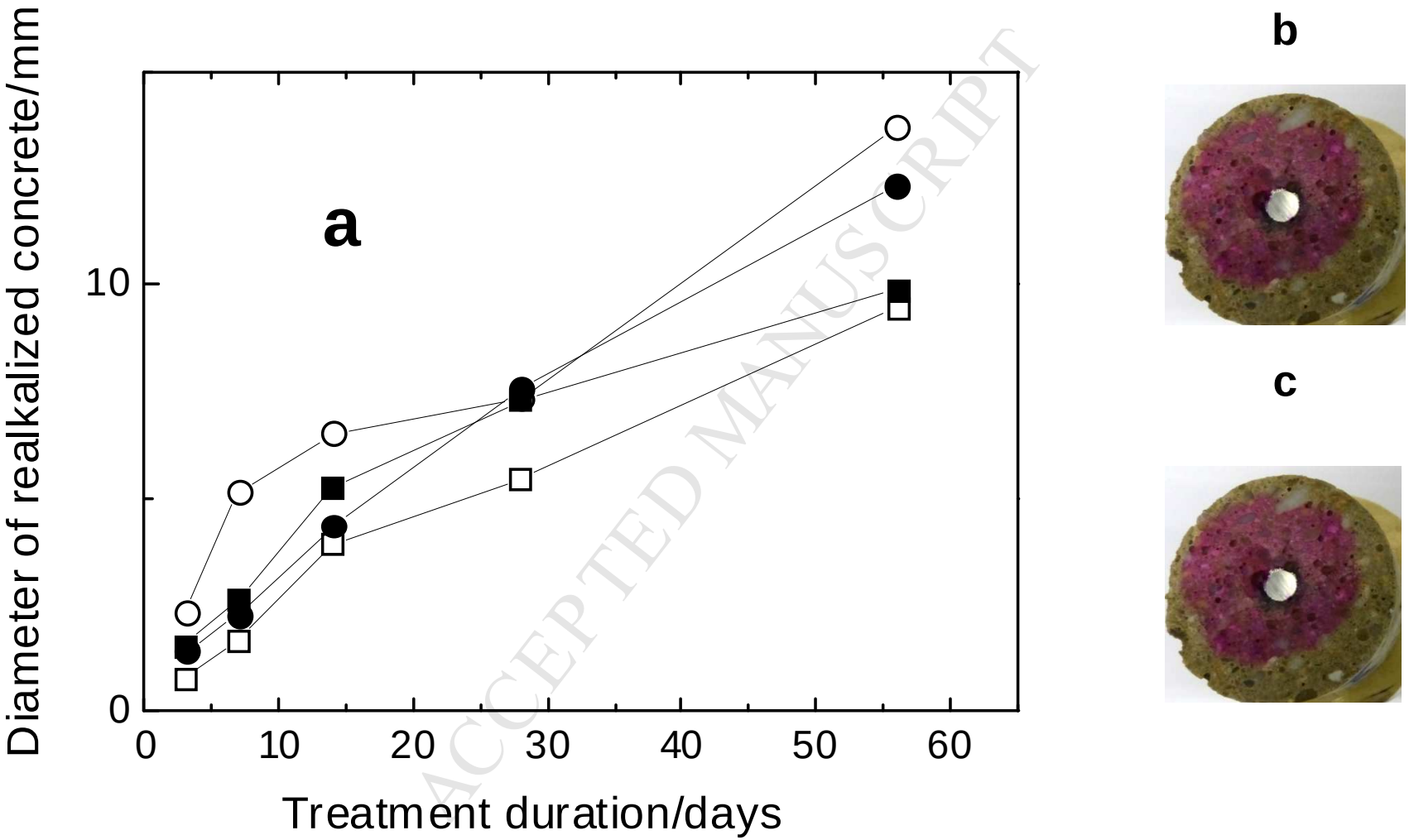

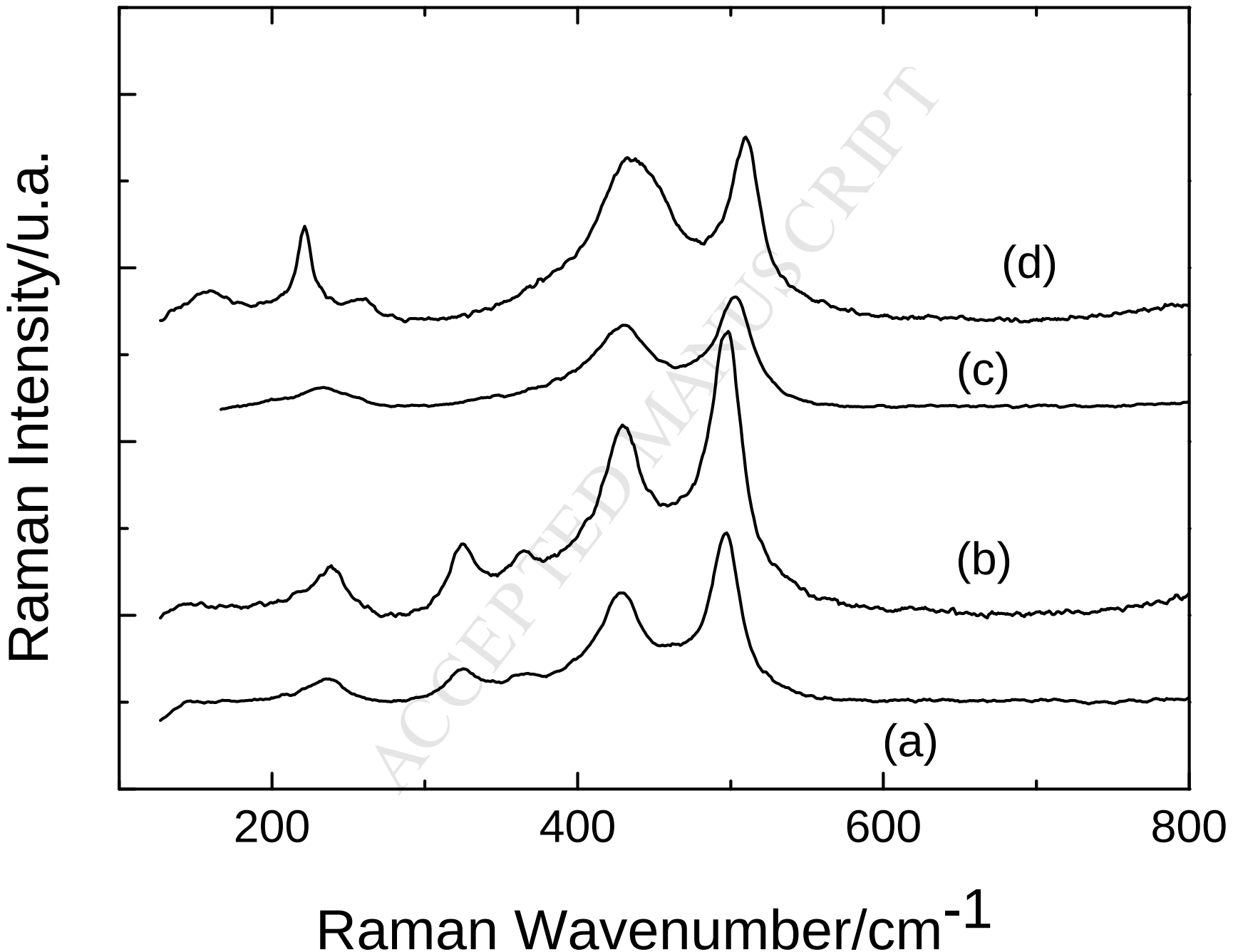

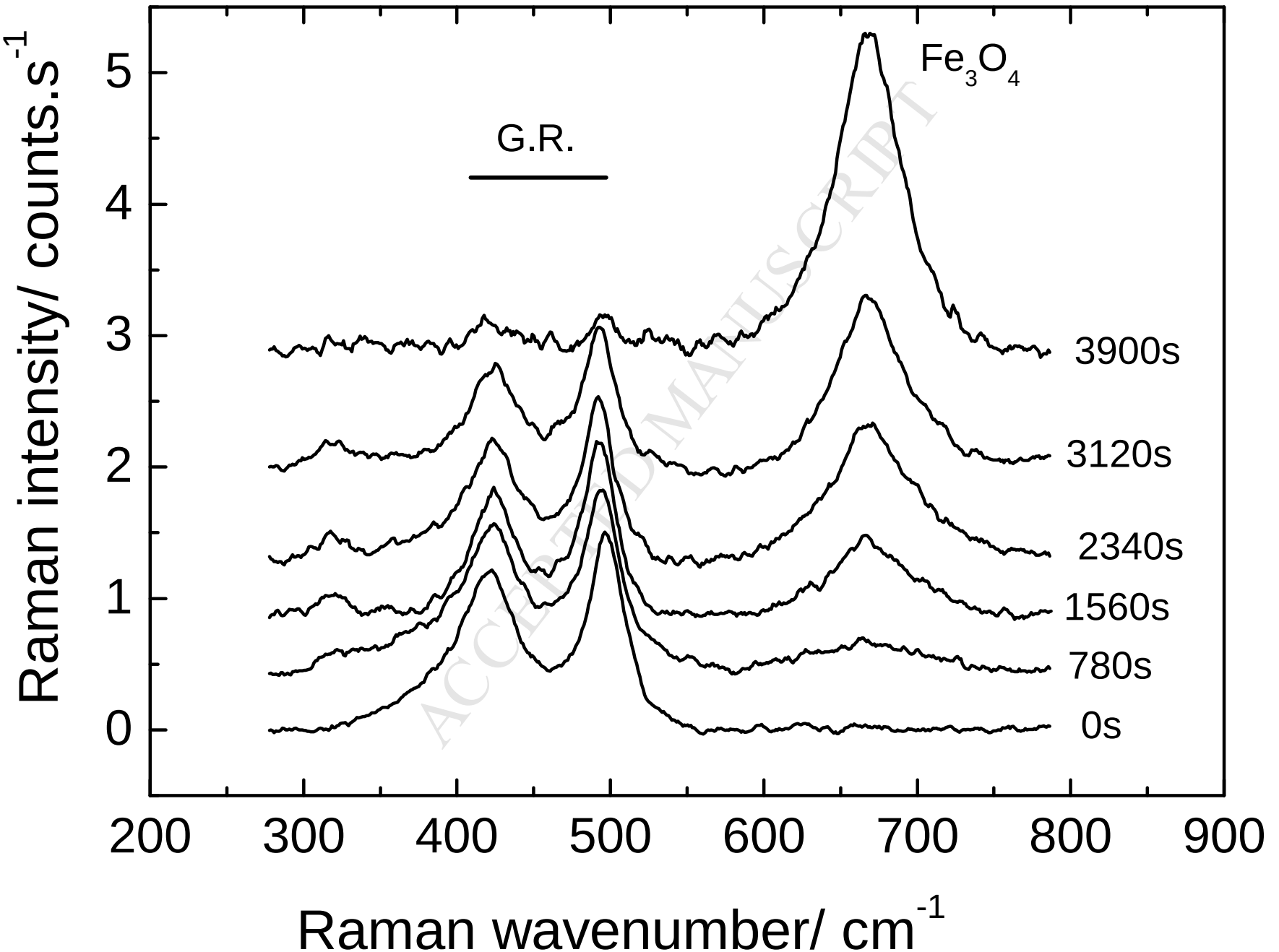

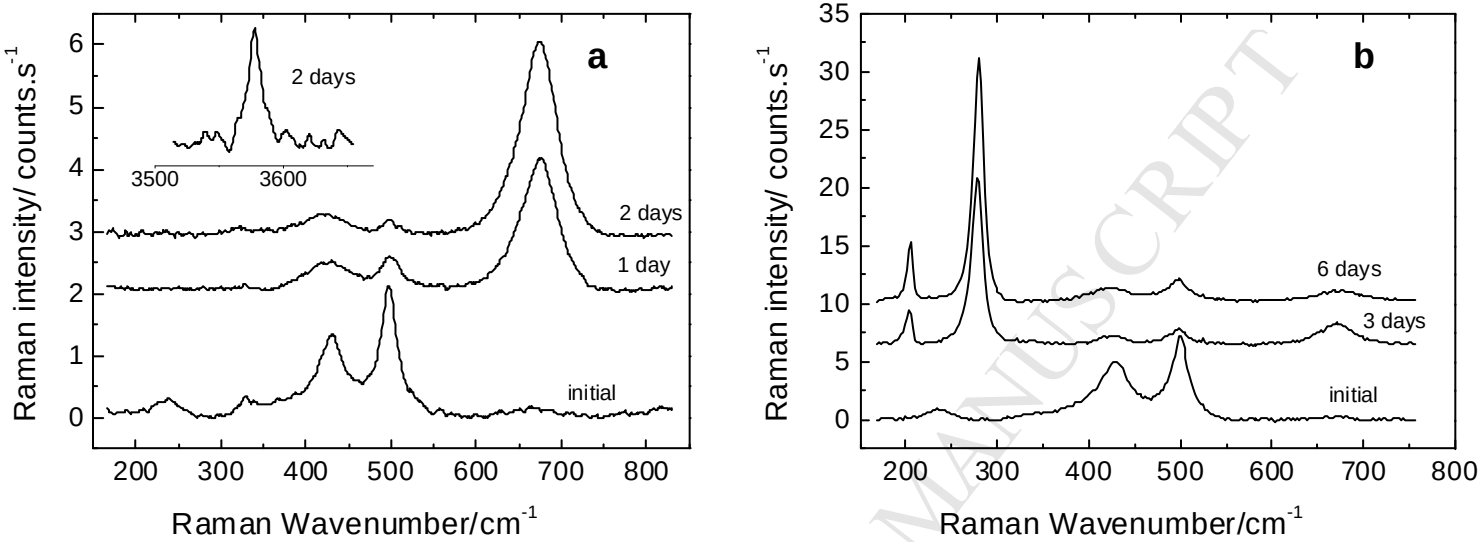

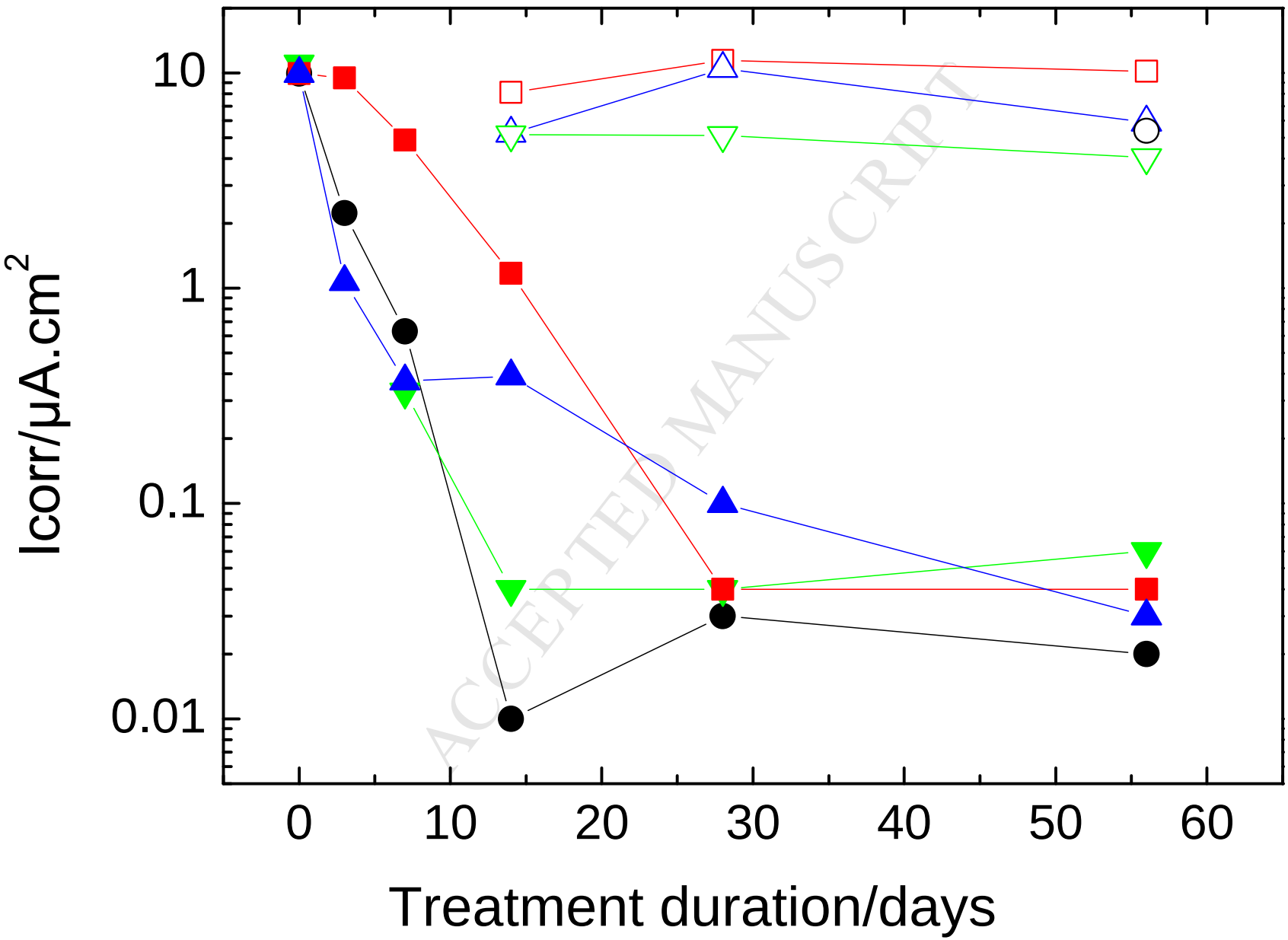

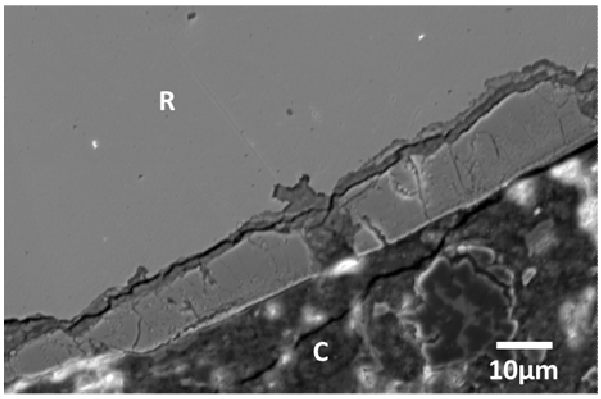

a)

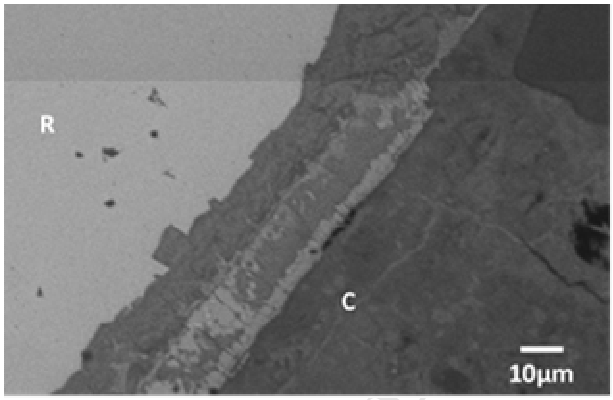

b)

Highlights

- High corrosion rate show the aggressiveness of combined contamination (Cl^-, CO_2).
- Electrochemical chloride treatment is provisionally efficient.
- Long term durability of ECE is questionable (pH increase is insufficient).